CHEMISTRY
A EUROPEAN JOURNAL

DOI: 10.1002/chem.200801043

Pt@MOF-177: Synthesis, Room-Temperature Hydrogen Storage and Oxidation Catalysis

Sebastian Proch,[a] Justus Herrmannsdörfer,[a] Rhett Kempe,*[a] Christoph Kern,[b] Andreas Jess,[b] Lena Seyfarth,[c] and Jürgen Senker[c]

Abstract: The gas-phase loading of $[Zn_4O(btb)_2]_8$ (MOF-177; H_3btb = 1,3,5-benzenetribenzoic acid) with the volatile platinum precursor $[Me_3PtCp']$ (Cp' = methylcyclopentadienyl) was confirmed by solid state ^{13}C magic angle spinning (MAS)-NMR spectroscopy. Subsequent reduction of the inclusion compound $[Me_3PtCp']_4$@MOF-177 by hydrogen at 100 bar and 100 °C for 24 h was carried out and gave rise to the formation of platinum nanoparticles in a size regime of 2–5 nm embedded in the unchanged MOF-177 host lattice as confirmed by transmission electron microscopy (TEM) micrographs and powder X-ray diffraction (PXRD). The room-temperature hydrogen adsorption of Pt@MOF-177 has been followed in a gravimetric fashion (magnetic suspension balance) and shows almost 2.5 wt% in the first cycle, but is decreased down to 0.5 wt% in consecutive cycles. The catalytic activity of Pt@MOF-177 towards the solvent- and base-free room temperature oxidation of alcohols in air has been tested and shows Pt@MOF-177 to be an efficient catalyst in the oxidation of alcohols.

Keywords: hydrogen storage · metal–organic frameworks · nanoparticles · oxidation · platinum

Introduction

Among the many types of porous solids, so-called porous coordination polymers or metal–organic frameworks (MOFs) have gathered special attention, due to their flexibility in pore size. This flexibility arises from the unique assembly of this type of solids. Organic linkers are connected through metal centres or inorganic metal clusters (SBUs = secondary building units) to form 3D frameworks.[1] By using bifunctional linkers we synthesised and characterised a variety of such porous 3D networks.[2] A special class of MOFs, basic zinc carboxylates, introduced by Yaghi et al.,[3,4] have been investigated extensively in gas storage applications[5–12] and as host lattices for the formation of nanoparticles.[13–18]

The development and introduction of a global hydrogen economy including hydrogen as onboard energy carrier for automobile applications require a safe way to store sufficient amounts of hydrogen.[19–22] Different approaches exist today in order to find suitable ways of hydrogen storage. Conventional storage in pressure tanks leads to considerable dangers and cryogenic transport of liquid hydrogen on the other hand yields a constant loss of H_2 through heat exchange.[19] Another way is the chemical modification of the H_2 molecule and the application of metal hydrides; mainly aluminium- and borohydrides are used.[23–36] Major disadvantages here lie in the liberation of the hydrogen and the regeneration of the hydride. A third way is based on the physisorption of hydrogen into porous solids. One class of these materials constitutes carbon nanotubes (CNTs).[37–42] Unfunctionalised CNTs show meagre hydrogen storage results at room temperature.[37,40] Another class are polymers showing intrinsic microporosity (PIMs), for example, PIM-1, can reach a storage capacity of 3.0 wt% H_2 at 77 K and 15 bar.[43] And finally a lot of attention has been paid to nanoporous metal–organic frameworks and their storage capacities. Although superior results are obtained at 77 K[44–48] the room temperature capacities are discouraging.[10,49,50]

[a] S. Proch, J. Herrmannsdörfer, Prof. Dr. R. Kempe
Lehrstuhl für Anorganische Chemie II
Universität Bayreuth
Universitätsstrasse 30, 95440 Bayreuth (Germany)
Fax: (+49) 921-55-2157
E-mail: kempe@uni-bayreuth.de

[b] Dr. C. Kern, Prof. Dr. A. Jess
Lehrstuhl für Chemische Verfahrenstechnik
Universität Bayreuth
Universitätsstrasse 30, 95440 Bayreuth (Germany)

[c] L. Seyfarth, Prof. Dr. J. Senker
Lehrstuhl für Anorganische Chemie I
Universität Bayreuth
Universitätsstrasse 30, 95440 Bayreuth (Germany)

Recently, a method was developed to increase the hydrogen-storage capacity of metal–organic frameworks (MOF-5 and IRMOF-8) through chemical bridging to platinum supported on activated carbon.[8,9,51,52] The underlying effect for this considerable increase of storage capacity (MOF-5 at 298 K and 100 bar: 0.4 wt% → 3.0 wt%) is called hydrogen spillover.[53,54] In general spillover describes the transport of an activated species (not necessarily hydrogen) from one surface (for instance, metallic surface) to another surface, that does not form or adsorb that species under the same conditions (acceptor surface). This process can be continued to more than one surface, which is called primary, secondary,… spillover.[8,9,51,52] The possibility to generate nanoparticles inside a MOF host lattice by means of MOCVD or solution infiltration techniques[13–18] led us to the idea of using a MOF as primary spillover acceptor.[8,9,51,52] Since MOF-177 has the highest adsorption of hydrogen so far at 77 K[55] Pt@MOF-177 seemed to be a promising candidate for hydrogen adsorption at room temperature.

Interesting applications of supported nanoparticles lie in the field of heterogeneous catalysis, including hydrogenation,[56–61] C–C coupling[62–69] or oxidation reactions.[70–75] The selective oxidation of alcohols yielding aldehydes and ketones is a highly important reaction and the developments of recent years tend to "green" chemistry reactions employing dioxygen or even air as an oxidant accompanied by mild reaction conditions (solvent-free, base-free). Most of the oxidation reactions are carried out at elevated temperatures between 80 °C[76,77,78] and 160 °C.[70] Room-temperature systems are quite rare.[72,75] Systems yielding the highest known TONs/TOFs for the oxidation of 1-phenylethanol include Pd/HAP-0 (hydroxyapatite-supported palladium nanoclusters) (TON: 236,000; TOF: 9,800 h^{-1} at 160 °C),[79,80] Au/CeO_2 (TON: 250,000; TOF: 12,500 h^{-1} at 160 °C),[81,82] Au/$Pd-TiO_2$ (Pd_{shell}–Au_{core} particles immobilised on titania) (TOF: 269,000 h^{-1} at 160 °C)[70] and gallium/aluminium oxide supported gold nanoparticles (TOF: 25,000 h^{-1} at 160 °C)[74] and work at temperatures well above 100 °C. A room-temperature oxidation catalyst applying air as an oxidizing agent was recently introduced by Miyamura et al.[72] based on polymer-incarcerated gold (PI–Au). It requires the addition of K_2CO_3 as a base[83] and oxidises aromatic and aliphatic alcohols smoothly to the corresponding aldehydes and ketones. Also recently Au/Pt@SPB (spherical polyelectrolyte brushes) was introduced as a room-temperature oxidation system and showed that pure platinum nanoparticles were able to oxidise alcohols at room-temperature with the addition of K_2CO_3 in water.[75] So it was chosen to apply MOF-177-supported nanoparticles as catalysts for the solvent- and base-free oxidation of alcohols at room-temperature.

Abstract in German: *Die mittels Sublimation durchgeführte Beladung von $[Zn_4O(btb)_2]_8$ (MOF-177; H_3btb = 1,3,5-Benzenetribenzoesäure) mit dem gut flüchtigen Platinprecursor $[Me_3PtCp']$ (Cp′ = Methylcyclopentadienyl) wurde durch ^{13}C-(MAS)-NMR-Spektroskopie belegt. Die nachgeschaltete Reduktion der Einschlussverbindung $[Me_3PtCp']_4$@MOF-177 durch H_2 wurde bei 100 bar und 100 °C durchgeführt. Sie führte zur Ausbildung von Platin-Nanopartikeln mit einer Grössenverteilung von 2 bis 5 nm, eingebettet im nahezu unveränderten MOF-177-Gastgitter, wie mittels Transmissionselektronenmikroskopie (TEM) und Pulverdiffraktometrie nachgewiesen werden konnte. Die Raumtemperatur-Wasserstoff-Aufnahme von Pt@MOF177 wurde gravimetrisch verfolgt (Magnetwaage) und es wurde eine Beladung von 2.5 Gewichts% im ersten Zyklus beobachtet, die jedoch in den Folgezyklen auf 0.5 Gewichts% sank. Die katalytische Aktivität von Pt@MOF-177 in der lösemittel- und basenfreien Raumtemperatur-Oxidation von Alkoholen mit Luftsauerstoff wurde untersucht und es zeigte sich das Pt@MOF177 ein effizienter Alkoholoxidationskatalysator ist.*

Experimental Section

Analytical and spectroscopic methods: Elemental analysis was performed by OrgaLab GmbH, Zirndorf Germany. The measurements were performed by standard protocols employing digestion in $HNO_3/HCl/H_2O_2$ and inductively coupled plasma mass spectrometry (ICP-MS).

GC analyses were performed by using an Agilent 6890N gas chromatograph equipped with a flame ionisation detector (FID) and an Agilent 19091 J-413 FS capillary column using dodecane as internal standard.

All X-ray powder diffractograms were recorded by using a STOE-STADI-P-diffractometer (CuK_α radiation, 1.54178 Å) in θ-2θ-geometry and with a position sensitive detector. All powder samples were introduced into glass capillaries ($\varnothing$ = 0.7 mm, Mark-tubes Hilgenberg No. 10) in a glove box and sealed prior to the measurements.

Solid-state ^1H and ^{13}C-MAS-NMR spectra were measured with a conventional impulse spectrometer Avance II (Bruker) operating with a resonance frequency of 300 MHz for ^1H (B_0 = 7.0 T). The samples were placed in zirconia rotors with a diameter of 4 mm (^{13}C) and 2.5 mm (^1H) and mounted in standard double-resonance MAS probes (Bruker). The rotation frequencies ν_{rot} varied between 7 kHz and 12 kHz for the ^{13}C spectra and were set to 30 kHz for the proton data. ^1H and ^{13}C resonances are reported with respect to TMS.

We acquired ^1H and ^{13}C-MAS-NMR data by exciting the FID with three back-to-back 90 degree impulses.[84] The sequence is designed to eliminate unwanted spectral contributions coming from the probe. The 90 degree impulse length was adjusted to 3 μs and the recycle delay was chosen to guarantee total rebuild of magnetisation due to spin-lattice relaxation. Alternatively, for faster scanning ^{13}C-MAS spectra were acquired using ^1H–X cross-polarisation double resonance experiments with contact times t_H between 1 ms and 10 ms. We employed a ramped cross-polarisation sequence[85] by linearly reducing the ^1H radiation power from 100% to 50%. The FIDs for all ^{13}C spectra were recorded using broadband proton decoupling with a SPINAL64 sequence.[86]

The transmission electron microscopy (TEM) was carried out by using a LEO 9220 (200 kV) instrument. The sample was suspended in chloroform and sonicated for 30 min. Subsequently a drop of the suspended sample was placed on a grid (Plano S 166–3).

Reactants and solvents: All manipulations and chemical reactions were conducted by inert atmosphere and glove box techniques (N_2, H_2O, O_2 < 0.1 ppm). All solvents were catalytically dried, deoxygenated and saturated with Argon using reflux conditions.

Starting materials synthesis: 1,3,5-Benzene-tri-benzoic acid (H_3btb) was prepared by using literature procedures.[87] MOF-177 was obtained by the method of Yaghi et al.[55] Colourless to pale yellow crystals of ≈5 mm

edge length were solvent exchanged in chloroform for one week by Soxhlet extraction. The off-white crystals were dried in dynamic vacuo (5×10^{-5} mbar) at 125 °C for 3 d. The crystals were ground to powder, characterised by using PXRD and stored in a glove box under inert atmosphere. MOF-177 powder was introduced into a glass capillary (ø = 0.7 mm, Mark-tubes Hilgenberg No. 10) under an inert atmosphere in a glove box and sealed. PXRD reflections and intensities were as follows: 2θ(%): 5.5 (79), 5.9 (77), 6.2 (100), 7.6 (28), 7.9 (27), 9.5 (17), 10.4 (18), 11.3 (17) 13.9 (11), 15° (11). The diffraction pattern fits the PXRD of activated MOF-177 from the literature.[91]

Infiltration of [Me_3PtCp'] into MOF-177, preparation of [Me_3PtCp']$_4$@MOF-177: In a typical experiment, a sample of 300 mg (0.26 mmol) dry, activated MOF-177 powder and 500 mg (1.6 mmol) [Me_3PtCp'] were placed in a two-chamber-tube separated by a glass frit and were kept at 35 °C in a 5×10^{-5} mbar (diffusion pump) static/dynamic (each hour the vacuum was renewed) vacuum for 12 h. The procedure yielded an off-white powder, which was stored under inert conditions in a glove box. Yield: 625 mg (97% based on Pt). ^{13}C-MAS-NMR (direct excitation): $\delta = -17.0$ ($(CH_3)_3$Pt), 12.4 (η^5-$C_5H_4CH_3$), 92.1 (C_b), 96.4 (C_a), 114.7 (C_c), 130.2 (C1–C6), 176.0 ppm (COO^-).

Preparation of Pt@MOF-177, quantitative hydrogenolysis of [Me_3PtCp'] in MOF-177: A sample of 300 mg [Me_3PtCp']$_4$@MOF-177 was placed in a steel autoclave (Parr) and was reduced in a hydrogen atmosphere (100 bar, 100 °C) for 1 d and yielded a black powder. To remove traces of the former ligands, the material was evacuated for 24 h at 5×10^{-5} mbar (125 °C). The powder was characterised by using PXRD and stored in a glove box under inert atmosphere. Pt@MOF-177 powder was placed into a glass capillary (ø = 0.7 mm, Mark-tubes Hilgenberg No. 10) under inert atmosphere in a glove box and sealed. PXRD reflections and intensities were as follows: 2θ (%) = 5.5 (84), 5.9 (100), 6.2 (63), 7.6 (21), 7.9 (20), 9.5 (20), 10.4 (14), 11.3 (14) 13.9 (14), 15 (14), 39.9 (84), 46.5 (38), 67.7° (24). ICP-MS (wt.%) calculated for Pt@MOF-177: Pt 41; found: Pt 43 ± 4; ^{13}C-MAS-NMR: δ = 131.4 (C1–C6), 175.8 ppm (COO^-).

Hydrogen adsorption at room-temperature: 226 mg of Pt_4@MOF-177 (43 wt.%) were transferred to a magnetic suspension balance (Rubotherm) in air (exposure ≈5 min) and degassed at 8×10^{-3} mbar and 150 °C until a constant mass was achieved (Figure 1).

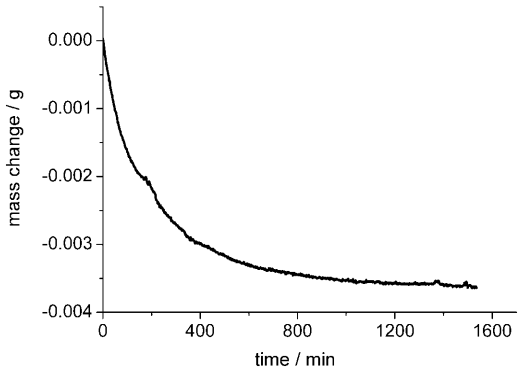

Figure 1. Weight loss of Pt@MOF-177 at 150 °C and 8×10^{-3} mbar (226 mg sample).

Magnetic suspension balances allow extremely precise measurements of mass changes to be obtained and can be effected on samples under defined environments. Additionally, the suspension balance is capable of measuring the gas density at any time so no buoyancy correction, employing constitutional equations, is needed. Two measurements are conducted. In the first measurement (MP1) only the mass change of the sample (incl. sample holder) was determined. In a second step (MP2) the mass change owing to buoyancy of an inert titan sinker was ascertained. The combination of both measurements enables the determination of the mass change owing to sorption by using Equation (1):

$$\Delta m_{ads} = \Delta m_{MP1} - \frac{V_{sample}}{V_{titan\ cylinder}} \Delta m_{MP2} \quad (1)$$

If the volume ratio between sample (sample + sample holder) and the titan sinker is known, the mass change owing to sorption can be determined. The volume ratio is found by calibration by a non adsorbing gas (Helium 4.6). In that case Equation (2) holds and Equation (3) is valid at any time during the measurement:

$$\Delta m_{ads} = 0 : 0 = \Delta m_{MP1} - \frac{V_{sample}}{V_{titan\ cylinder}} \Delta m_{MP2} \quad (2)$$

$$\Delta m_{MP1} = \frac{V_{sample}}{V_{titan\ cylinder}} \Delta m_{MP2} \quad (3)$$

Now the slope of a plot of Δm_{MP1} vs. Δm_{MP2r} yields the volume ratio (Figure 2), a ratio of 0.505 ± 0.005 was determined. Subsequently the sample chamber was evacuated and three consecutive cycles of adsorption at a constant pressure of 144 bar at 298 K were carried out in a pure hydrogen atmosphere (Hydrogen 5.0). As soon as complete saturation was achieved the hydrogen was removed in vacuo at 8×10^{-3} mbar (Figures 3 and 4).

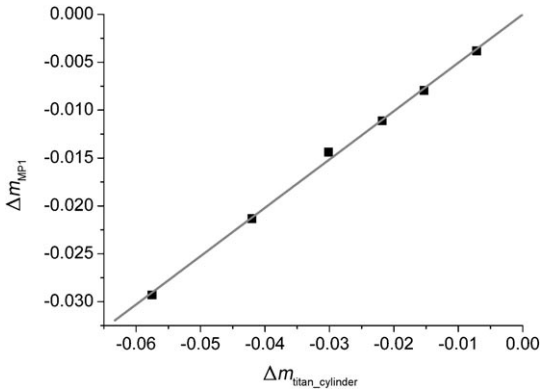

Figure 2. Calibration of the Pt@MOF-177 sample with helium as non-adsorbing gas.

Oxidation of alcohols using Pt@MOF-177 as catalyst: 10 mg Pt@MOF-177 (4×10^{-4} mmol) were suspended in 1 mL of the alcohol or 1 g in 4 mL thf and stirred for 24 h at room temperature in air. The conversion was checked by GC using dodecane as internal standard.

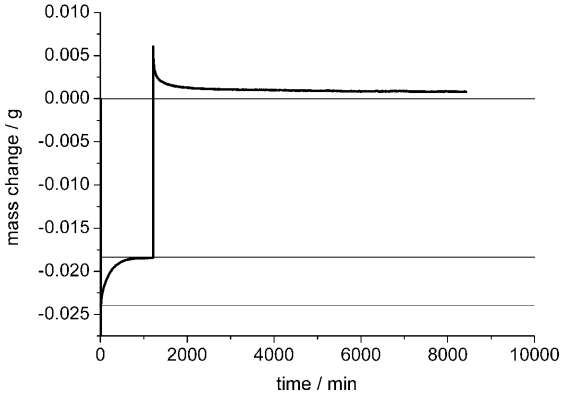

Figure 3. Adsorption and desorption of hydrogen from Pt@MOF-177 (223 mg sample) in the first cycle at 298 K and 143 mbar; desorption: 8×10^{-3} mbar and 298 K, desorption does not take place at ambient pressure.

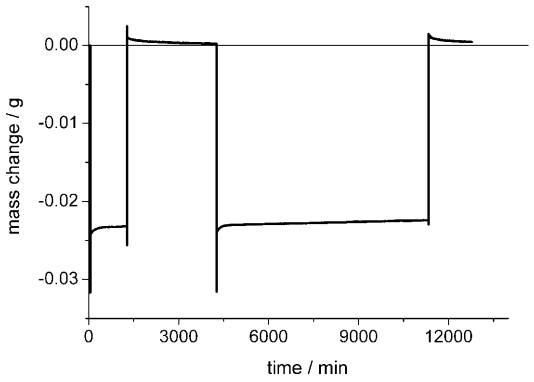

Figure 4. Adsorption and desorption of hydrogen from Pt@MOF-177 (223.9 mg sample) in the second and third cycle at 298 K and 144 mbar; desorption: 8×10^{-3} mbar and 298 K.

For the oxidation of benzyl alcohol 100 mg of Pt@SPB were suspended in 40 mL of benzyl alcohol and 2 mL of dodecane were added. Samples were taken via cannula to keep the catalyst inside the suspension while taking aliquots. After 48 h, a conversion of 50% was observed. For a second run the catalyst was filtered off, stirred in dry chloroform (24 h) and dried in vacuo for another 24 h at 125°C.

Results and Discussion

Loading of MOF-177 with [Me_3PtCp']: To generate platinum nanoparticles inside MOF-177 [Me_3PtCp'] has been chosen as a precursor. It is commercially available and very volatile, it sublimes at ambient conditions[88] and decomposes in a hydrogen atmosphere to Pt(0), methylcyclopentadiene and methane, which can be easily removed. Loading of MOF-177 was performed in a static/dynamic vacuum (5×10^{-5} mbar) at 35°C (above the melting point of [Me_3PtCp']) for 12 h. Upon loading with the white crystals of [Me_3PtCp'] the MOF-177 powder kept its off-white colour. The direct excitation ^{13}C-MAS-NMR spectrum of the inclusion compound [$Me_3PtCp']_4$@MOF-177 is shown in comparison to pure MOF-177 in Figure 5. The carbon resonance signals of the btb (H_3btb = 1,3,5-benzenetribenzoic acid) moiety of MOF-177 were found at $\delta = 176.0$ ppm (COO^-) and the remaining signals in a multiplet at $\delta = 130.2$ ppm. The signals of [Me_3PtCp'] are observed at $\delta = -17.0$ (($CH_3)_3$Pt), 12.4 (η^5-$C_5H_4CH_3$), 92.1 (C_b), 96.4 (C_a), 114.7 ppm (C_c). These signals originate from intact [Me_3PtCp'] and are very close to the signals known from this compound in solution.[14,88] From the direct excitation ^{13}C-MAS-NMR spectrum the number of molecules per formula unit of MOF-177 can be determined through signal integration (not possible in CP spectra) to 4.0($\pm$0.3), denoting that 4 molecules of [Me_3PtCp'] are included in one pore of MOF-177.

Quantitative hydrogenolysis of [$Me_3PtCp']_4$@MOF-177 to give Pt@MOF-177

Synthesis and analytical characterisation: To achieve quantitative hydrogenolysis of [$Me_3PtCp']_4$@MOF-177 the compound was kept in a 100 bar hydrogen atmosphere at 100°C for 24 h. After that period all decomposition traces of [Me_3PtCp'] were removed in vacuo at 125°C for 24 h. The procedure yielded a black powder. The ^{13}C-MAS-NMR spectrum of the reduced compound matches the spectrum of pure MOF-177 (Figure 6) and shows that no traces of volatile decomposition products from [Me_3PtCp'] are present and a hydrogenation of the btb-linkers has not taken place. An ICP-MS measurement of the platinum content of Pt@MOF-177 reveals 43 wt% of platinum, which is close to the predicted 41 wt% arising from [$Me_3PtCp']_4$@MOF-177.

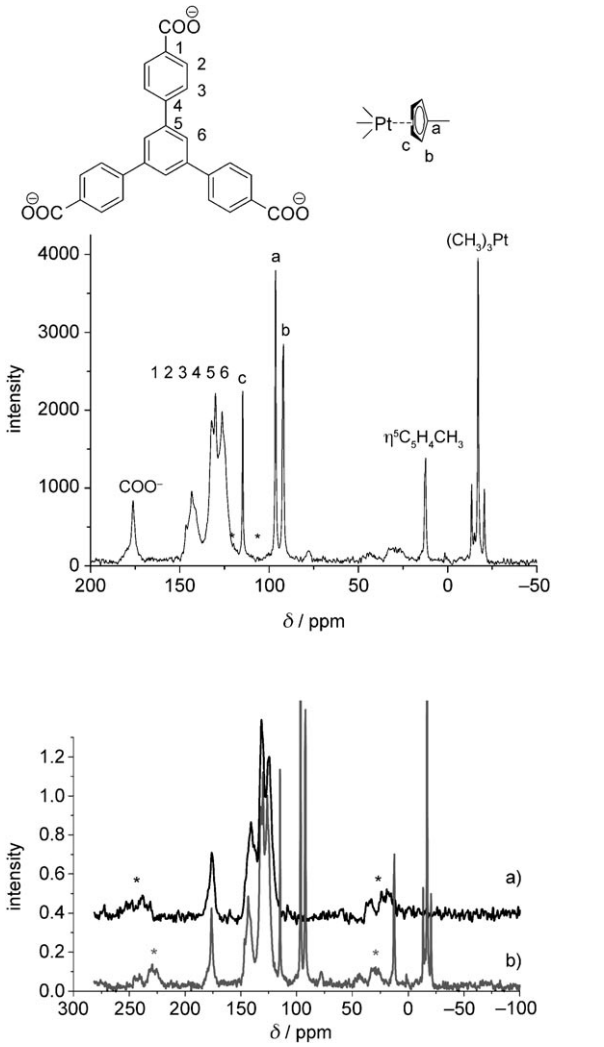

Figure 5. Top: ^{13}C-MAS-NMR (direct excitation) of [$Me_3PtCp']_4$@MOF-177. Bottom: comparison between a) the pristine MOF-177 and b) the inclusion compound. The asterisks denote spinning side bands.

PXRD and TEM studies of Pt@MOF-177: Powder X-ray diffraction (PXRD) measurements of Pt@MOF-177 show no change in the region $2\theta < 20°$, the typical region of reflections from the MOF-177 host lattice. New reflections appear at $2\theta = 39.9$, 46.5, 67.7° corresponding to the incorporated platinum (Figure 7). It exhibits the characteristic diffraction peaks for the face-centred cubic crystal structure of plati-

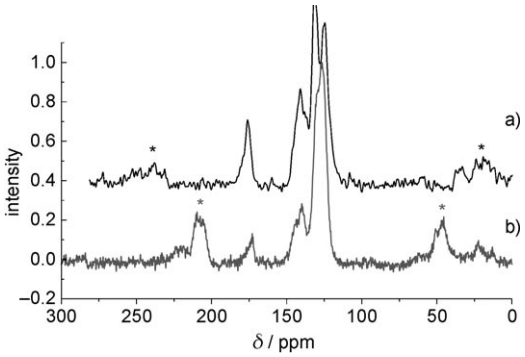

Figure 6. ^{13}C-MAS-NMR of a) pristine MOF-177 and b) Pt@MOF-177. The asterisks denote spinning side bands.

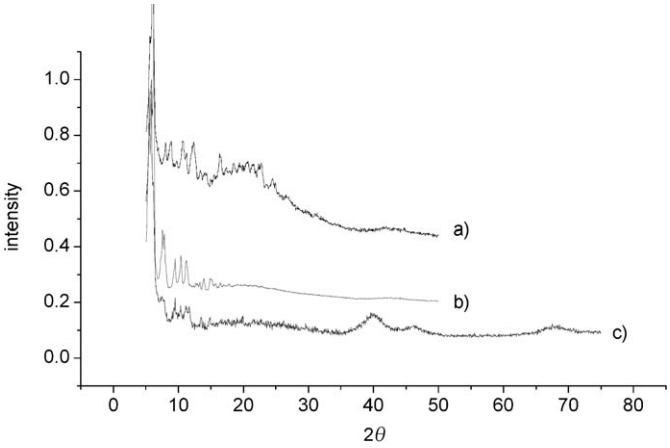

Figure 7. PXRD of a) as-synthesised MOF-177, b) guest-free MOF-177 (SSA = 5600 $m^2 g^{-1}$, accessible micropore volume = 1.69 $cm^3 g^{-1}$, SSA = specific surface area) and c) Pt@MOF-177 (SSA = 867 $m^2 g^{-1}$, accessible micropore volume = 0.39 $cm^3 g^{-1}$).

num.[89] The MOF-177 host lattice remains unchanged in the process of loading and reducing of the platinum precursor [Me_3PtCp']. From the reflection at 39.9° with an FWHM of 5° an average size of the platinum nanoparticles of 2.2 nm can be calculated by using the Scherrer equation.[90] The average pore size matches very closely the pore size of MOF-177.[91]

The TEM images of Pt@MOF-177 (Figure 8) show as well as the PXRD pattern, that the porous host structure is still intact after loading and short exposition time to air (around 10 min). The images visualise that only few cavities within the MOF-177 host lattice are filled with Pt nanoparticles. The size of these particles is mainly between 2 and 3 nm. The TEM investigations also show that agglomeration of Pt particles occurs, because particles with up to 5 nm size can be found (Figure 8, right). Furthermore no significant agglomeration of platinum on the edges of the crystallites is observed (Figure 8, left, middle).

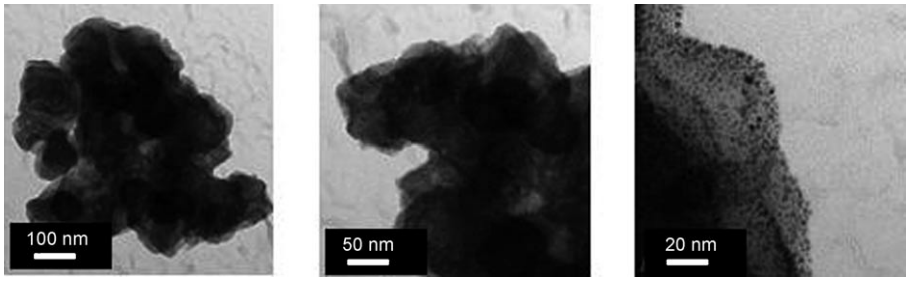

Figure 8. TEM images of Pt@MOF-177 (derived from hydrogenolysis of [Me_3PtCp']$_4$@MOF-177 at 100 °C and 100 bar H_2 for 24 h).

Hydrogen-storage properties of Pt@MOF-177: The hydrogen-storage features of Pt@MOF-177 were investigated in a gravimetric fashion by means of a magnetic suspension balance at room temperature.[40] MOF-177 exhibits the highest hydrogen uptake at 77 K for metal–organic frameworks so far.[55] The room-temperature uptake however is rather low, as is the case for most metal–organic frameworks.[10,92] A method to increase the room-temperature uptake of metal–organic frameworks through spillover was developed by Li et al.[8,9,52] We reasoned the same effect to originate from platinum particles directly grown into the porous host as in the chemically bridged structure synthesised by Li et al.,[9] where the platinum spillover source is immobilised on activated carbon. The metal surface of the platinum particles is likely to activate (dissociate) the hydrogen molecules, which is a fast process.[53,54] The diffusion of the activated hydrogen from the metal surface to the MOF surface on the other hand is an endothermic and therefore slow process,[53,54] leading to the expectation of an overall slow hydrogen adsorption. The Pt@MOF-177 sample was exposed to a hydrogen atmosphere of 144 bar at room-temperature and the mass change due to adsorption was followed over time. The assumption of a constant pressure holds at any time during the experiment, because the volume of hydrogen is huge (3×10^{-1} L) compared to the sample (8×10^{-5} L, 200 mg, density determination by means of a suspension in chloroform; 2.5 g × cm^{-3}). A constant pressure leads to constant buoyancy during the measurement. This in turn means that there is no buoyancy contribution to the mass change.[40] that is, the mass change is directly due to the adsorption and no calibration is needed. However, it was done anyway and the corrected and directly measured uptakes were the same. The concentration of the hydrogen remains constant unlike in volumetric measurements (Sievert's apparatus) and the reaction order of the adsorption reaction is reduced (pseudo order), that is, the curves shown in Figure 9 are the pseudo adsorption kinetics of Pt@MOF-177 at room-temperature and 144 bar hydrogen pressure. The high uptake of 2.5 wt % in the first cycle drops down to a somewhat disillusioning 0.5 wt %, which is close to the room-temperature uptake of pure MOF-177

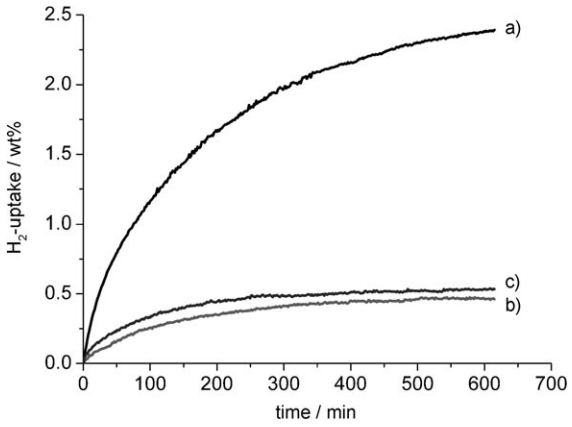

Figure 9. Pt@MOF-177 spillover curves three times in a row in a pure hydrogen atmosphere; a) first cycle, 298 K, 143 bar; b) second cycle, 298 K, 144 bar; c) third cycle, 298 K, 144 bar.

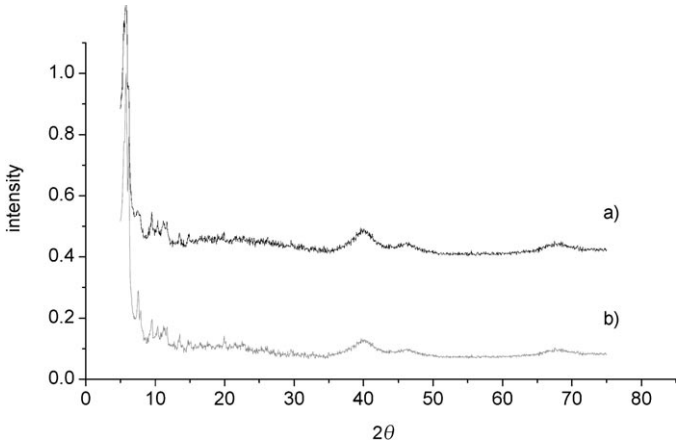

Figure 11. PXRD of a) Pt@MOF-177 and b) Pt@MOF-177 after hydrogen storage.

found by Miller et al.[92] However, following the desorption curve of the first cycle in high vacuum at room temperature—standard pressure desorption does not take place (Figure 3)—shows that not all adsorbed hydrogen is liberated (0.9 mg remain inside the host structure), that is, the hydrogen uptake is not completely reversible, but it becomes completely reversible in the second and third cycle after the drop in hydrogen uptake (Figure 4). This mass gain does not originate from either hydrogenation of the btb-linkers or the liberation of free H_3btb (^{13}C NMR of H_3btb shows the carboxylate at 169 ppm)[87] and destruction of the Zn_4O-clusters as found by ^{13}C-MAS-NMR (Figure 10). Also the

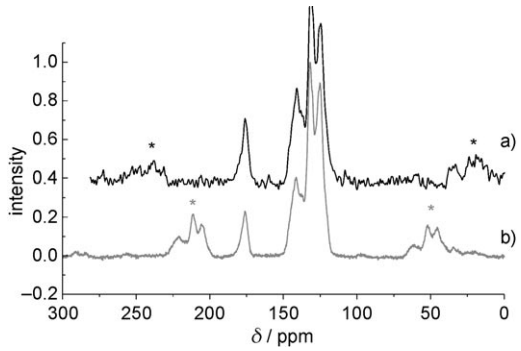

Figure 10. ^{13}C-MAS-NMR of a) pristine MOF-177 and b) Pt@MOF-177 after hydrogen storage. The asterisks denote spinning side bands.

porous host structure is not destroyed by the spillover process as confirmed by PXRD before and after hydrogen adsorption (Figure 11). The behaviour of the Pt@MOF-177 in the hydrogen-storage process is comparable to palladium immobilised in a carbon material: Pd/CT (C*T*=carbon template).[93] Here the storage capacity also drops down at room temperature in the second cycle but remains constant thereafter. This loss in uptake is attributed to the formation of palladium hydrides that are not desorbed at room-temperature as confirmed by TDS (thermal-desorption mass spectroscopy), which shows a desorption peak at 300 °C. The ^{1}H-MAS-NMR before and after hydrogen storage (Figure 12) shows no additional peaks after three storage cycles. The signals of H_3btb at $\delta = 7.95$ and 8.52 ppm are accompanied

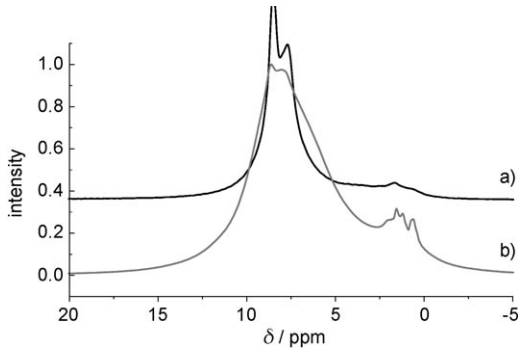

Figure 12. ^{1}H-MAS-NMR of a) Pt@MOF-177 and b) Pt@MOF-177 after hydrogen storage.

by low intensity signals between $\delta = 0$–2 ppm that might stem from the reduction process of the MOCVD precursor or from short exposition to air in both cases. The btb-linker signals however show a significant additional amount of intensity which might originate from a new signal appearing at $\delta = 6$ ppm due to platinum hydrides, which is derived from the signal shape and its chemical shift, they are similar to the hydrides in Mg_2NiH_x and MgH_x.[94]

Pt@MOF-177 as catalysts for room-temperature alcohol oxidation: As displayed in recent literature, platinum nanoparticles are efficient catalysts for the oxidation of alcohols.[75,95] It was decided to test the catalytic activity as well as the recyclability of Pt@MOF-177 for a variety of alcohols (Scheme 1). The base-free room-temperature approach was carried out for different alcohols including allylic and aliphatic substrates (Table 1). Although allylic alcohols, except iodo- and bromo-substituted benzyl alcohols, are oxidised smoothly with high selectivity (owing to mild reaction condi-

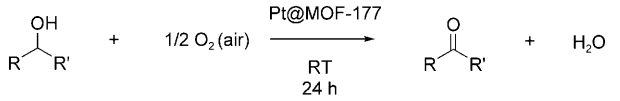

Scheme 1. Catalytic oxidation of alcohols employing Pt@MOF-177 as heterogeneous catalyst.

tions), saturated aliphatic and cyclic alcohols are unreactive under the conditions applied. The inactivity towards bromo- and iodo-substituted benzylic alcohols is traced back to the ability of Pt to insert into the C–Br and C–I bond and the resultant blocking of the particle surface.

The recyclability was tested using benzyl alcohol as a substrate. After the first cycle the Pt@MOF-177 nanocomposite was filtered off, washed with chloroform, dried in vacuo and investigated by XRD (Figure 13). The XRD pattern shows no reflections in the MOF-177 range (5–20 2θ) anymore. A breakdown of the MOF host lattice has occurred. A second cycle with the same catalysts shows almost no activity (only trace amounts of benzaldehyde) in the oxidation process. This can be explained by the now inaccessible platinum particles in the destroyed host. Similar observations have been made by Sabo et al. on Pd@MOF-5 used for the hydrogenation of styrene.[18] MOFs including the Zn_4O cluster as SBUs tend to be water sensitive[96] and, since water is produced as byproduct in the oxidation process (Scheme 1), the MOF host lattice might be destroyed.

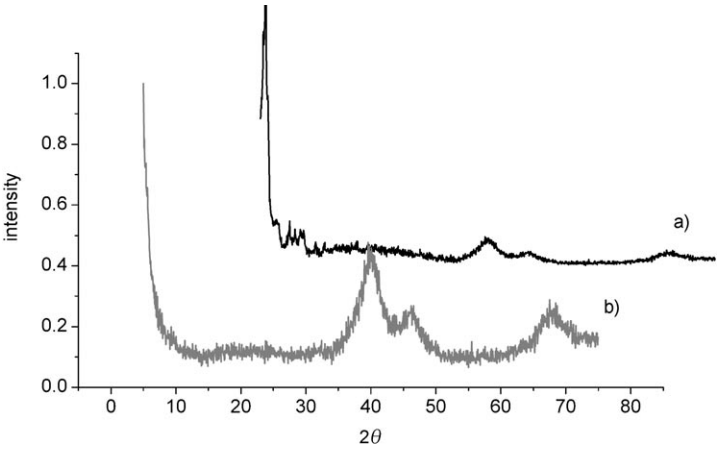

Figure 13. PXRD of a) Pt@MOF-177 and b) Pt@MOF-177 after oxidation catalysis.

Table 1. Catalytic room-temperature oxidation of alcohols by using Pt@MOF-177.

Entry	Alcohol	Ketone/Aldehyde	GC Conversion	TON
1	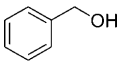	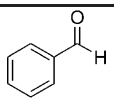	50 %	968
2	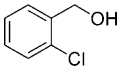	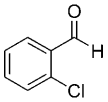	> 99 %	351
3	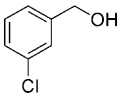	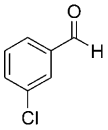	> 99 %	425
4	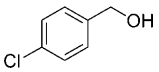	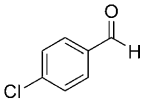	> 99 %	351
5	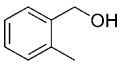	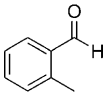	> 99 %	407
6	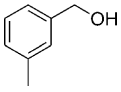	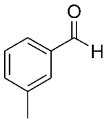	> 99 %	415
7	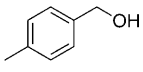	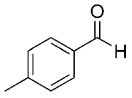	> 99 %	407
8	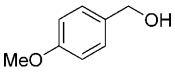	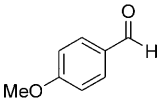	> 99 %	362
9	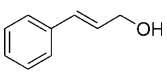	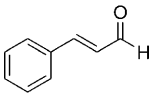	> 99 %	385

Conclusion

The generation of platinum nanoparticles in the MOF-177 host structure has been achieved by MOCVD methods employing $[Me_3PtCp']$ as a volatile precursor. The synthesis consists of a two step procedure in which initially the inclusion compound $[Me_3PtCp']_4$@MOF-177 is formed and characterised and subsequent hydrogenolysis gives rise to Pt@MOF-177. The prepared nanocomposite material has been characterised by PXRD, TEM and MAS-NMR to give a consistent view of the material. The average particle size of 2.2 nm derived from the PXRD reflections of platinum indicate the particles are formed inside the cavities of MOF-177 since the btb–btb distance in a single pore is 2.3–2.5 nm. TEM investigations revealed a similar average particle size, but also formation of larger particles. 2.5 wt % hydrogen uptake was

found for Pt@MOF-177 for the first cycle (144 bar and room temperature). The uptake however decreases in subsequent cycles to the uptake of MOF-177 alone (0.5 wt %).[92] The reason for this deactivation was investigated and the hydrogenation of the btb-linkers as well as the breakdown of the MOF-177 host structure were ruled out. The very high platinum content of 43 wt % of the composite material leads to a high density of 2.5 $g cm^{-3}$. The uptake in the first cycle leads to a storage capacity of 62.5 $g H_2 l^{-1}$ which is close to the density of liquid hydrogen of 70 $g H_2 l^{-1}$. Pt@MOF-177 catalyses the solvent- and base-free oxidation of allylic alcohols at room-temperature with air as an oxidant. Cinamyl alcohol and benzyl alcohol and its derivatives are oxidised smoothly under very mild conditions with TONs of up to 1000. The instability of the MOF-177 host at the applied conditions remains a problem (Figure 13). Especially problematic is the sensitivity of the MOF host towards water, which is produced in a stoichiometric way during the oxidation process. The application of more stable water-based MOF materials as hosts for nanoparticles could solve this problem.

Acknowledgements

The authors wish to thank M. Schrinner, Chair of Physical Chemistry I, University of Bayreuth for the TEM measurements, B. Putz, Chair of Inorganic Chemistry I, University of Bayreuth for the PXRD spectra of the composite material and S. Lutschinger, Chair of Inorganic Chemistry I, University of Bayreuth for many solid-state NMR measurements. This work was supported by NanoCat, an International Graduate Program within the Elitenetzwerk Bayern.

[1] For selected reviews please see: a) S. R. Batten, R. Robson, *Angew. Chem.* **1998**, *110*, 1558–1595; *Angew. Chem. Int. Ed.* **1998**, *37*, 1460–1494; b) O. M. Yaghi, H. Li, C. Davis, D. Richardson, T. L. Groy, *Acc. Chem. Res.* **1998**, *31*, 474–484; c) A. J. Blake, N. R. Champness, P. Hubberstey, W.-S. Li, M. A. Withersby, M. Schröder, *Coord. Chem. Rev.* **1999**, *183*, 117–138; d) M. J. Zaworotko, *Angew. Chem.* **2000**, *112*, 3180–3182; *Angew. Chem. Int. Ed.* **2000**, *39*, 3052–3054; e) M. Eddaoudi, D. B. Moler, H. Li, B. Chen, T. M. Reineke, M. O'Keeffe, O. M. Yaghi, *Acc. Chem. Res.* **2001**, *34*, 319–330; f) B. Moulton, M. J. Zawarotko, *Chem. Rev.* **2001**, *101*, 1629–1658; g) A. N. Khlobystov, A. J. Blake, N. R. Champness, D. A. Lemenovskii, A. G. Majouga, N. V. Zyk, M. Schröder, *Coord. Chem. Rev.* **2001**, *222*, 155–192; h) B. Moulton, M. J. Zawarotko, *Curr. Opin. Solid State Mater. Sci.* **2002**, *6*, 117–123; i) S. Kaskel, Handbook of Porous Solids **2002**, *2*, 1190–1249; j) C. Janiak, *Dalton Trans.* **2003**, *14*, 2781–2804; k) S. L. James, *Chem. Soc. Rev.* **2003**, *32*, 276–288; l) S. Kitagawa, R. Kitaura, S. Noro, *Angew. Chem.* **2004**, *116*, 2388–2430; *Angew. Chem. Int. Ed.* **2004**, *43*, 2334–2375.

[2] a) T. Schareina, R. Kempe, *Z. Anorg. Allg. Chem.* **2000**, *626*, 1279–1281; b) T. Schareina, C. Schick, B. F. Abrahams, R. Kempe, *Z. Anorg. Allg. Chem.* **2001**, *627*, 1711–1713; c) T. Schareina, C. Schick, R. Kempe, *Z. Anorg. Allg. Chem.* **2001**, *627*, 131–133; d) B. Schoknecht, R. Kempe, *Z. Anorg. Allg. Chem.* **2004**, *630*, 1377–1379; e) R. Kempe, *Z. Anorg. Allg. Chem.* **2005**, *631*,1038–1040.

[3] H. Li, M. Eddaoudi, M. O'Keeffe, O. M. Yaghi, *Nature* **1999**, *402*, 276–279.

[4] O. M. Yaghi, M. O'Keeffe, N. W. Ockwig, K. H. Chae, M. Eddaoudi, J. Kim, *Nature* **2003**, *423*, 705–714.

[5] M. Eddaoudi, J. Kim, R. Nathaniel, D. Vodak, J. Wachter, M. O'Keeffe, O. M. Yaghi, *Science* **2002**, *295*, 469–472.

[6] A. R. Millward, O. M. Yaghi, *J. Am. Chem. Soc.* **2005**, *127*, 17998–17999.

[7] J. L. C. Rowsell, J. Eckert, O. M. Yaghi, *J. Am. Chem. Soc.* **2005**, *127*, 14904–14910.

[8] Y. Li, R. T. Yang, *J. Am. Chem. Soc.* **2006**, *128*, 726–727.

[9] Y. Li, R. T. Yang, *J. Am. Chem. Soc.* **2006**, *128*, 8136–8137.

[10] B. Panella, M. Hirscher, H. Puetter, U. Mueller, *Adv. Funct. Mater.* **2006**, *4*, 520–524.

[11] A. G. Wong-Foy, A. J. Matzger, O. M. Yaghi, *J. Am. Chem. Soc.* **2006**, *128*, 3494–3495.

[12] J. L. C. Rowsell, O. M. Yaghi, *J. Am. Chem. Soc.* **2006**, *128*, 1304–1315.

[13] S. Hermes, M.-K. Schroeter, R. Schmid, L. Khodeir, M. Muhler, A. Tissler, R. W. Fischer, R. A. Fischer, *Angew. Chem.* **2005**, *117*, 6394–6397; *Angew. Chem. Int. Ed.* **2005**, *44*, 6237–6241.

[14] F. Schröder, D. Esken, M. Cokoja, M. W. E. van den Berg, O. I. Lebedev, G. Van Tendeloo, B. Walaszek, G. Buntkowsky, H.-H. Limbach, B. Chaudret, R. A. Fischer, *J. Am. Chem. Soc.* **2008**, *130*, 6119–6130.

[15] S. Hermes, D. Zacher, A. Baunemann, C. Woell, R. A. Fischer, *Chem. Mater.* **2007**, *19*, 2168–2173.

[16] S. Hermes, F. Schroeder, R. Chelmowski, C. Woell, R. A. Fischer, *J. Am. Chem. Soc.* **2005**, *127*, 13744–13745.

[17] S. Hermes, F. Schroeder, S. Amirjalayer, R. Schmid, R. A. Fischer, *J. Mater. Chem.* **2006**, *16*, 2464–2472.

[18] M. Sabo, A. Henschel, H. Froede, E. Klemm, S. Kaskel, *J. Mater. Chem.* **2007**, *36*, 3827–3832.

[19] L. Schlapbach, A. Züttel, *Nature* **2001**, *414*, 353–358.

[20] A. Züttel, *Mater. Res. Materials Today* **2003**, *6*, 24–33.

[21] R. Coontz, B. Hanson, *Science* **2004**, *305*, 957.

[22] http://www1.eere.energy.gov/hydrogenandfuelcells/pdfs/hydrogen_posture_plan.pdf.

[23] E. C. Ashby, P. Kobetz, *Inorg. Chem.* **1966**, *5*, 1615–1617.

[24] P. Claudy, B. Bonnetot, J.-P. Bastide, J.-M. Letoffe, *Mater. Res. Bull.* **1982**, *17*, 1499–1504.

[25] B. Bogdanovic, M. Schwickardi, *J. Alloys Compd.* **1997**, *253–254*, 1–9.

[26] B. Bogdanovic, R. A. Brand, A. Marjanovic, M. Schwickardi, J. Tolle, *J. Alloys Compd.* **2000**, *302*, 36–58.

[27] J. Huot, S. Boily, V. Guther, R. Schulz, *J. Alloys Compd.* **1999**, *283*, 304–306.

[28] R. A. Zidan, S. Takara, A. G. Hee, C. M. Jensen, *J. Alloys Compd.* **1999**, *285*, 119–122.

[29] C. M. Jensen, R. A. Zidan, N. Mariels, A. G. Hee, C. Hagen, *Int. J. Hydrogen Energy* **1999**, *24*, 461–465.

[30] B. Bogdanovic, M. Felderhoff, S. Kaskel, A. Pommerin, K. Schlichte, F. Schüth, *Adv. Mater.* **2003**, *15*, 1012–1015.

[31] D. L. Anton, *J. Alloys Compd.* **2003**, *356–357*, 400–404.

[32] P. Vajeeston, P. Ravindran, R. Vidya, H. Fjellvag, A. Kjekshus, *Appl. Phys. Lett.* **2003**, *80*, 2257–2259.

[33] A. Züttel, S. Rentsch, P. Fischer, P. Wenger, P. Sudan, P. Mauron, C. Emmenegger, *J. Alloys Compd.* **2003**, *356–357*, 515–520.

[34] A. Züttel, P. Wenger, S. Rentsch, P. Sudan, P. Mauron, C. Emmenegger, *J. Power Sources* **2003**, *118*, 1–7.

[35] R. Aiello, M. A. Matthews, D. L. Reger, J. E. Collins, *Int. J. Hydrogen Energy* **1998**, *23*, 1103–1108.

[36] A. M. Seayad, D. M. Antonelli, *Adv. Mater.* **2004**, *16*, 765–777.

[37] G. G. Tibbetts, G. P. Meisner, C. H. Olk, *Carbon* **2001**, *39*, 2291–2301.

[38] R. H. Baughman, A. A. Zakhidov, W. A. de Heer, *Science* **2002**, *297*, 787–792.

[39] M. Hirscher, M. Becher, *J. Nanosci. Nanotechnol.* **2003**, *3*, 3–17.

[40] A. Lan, A. Mukasyan, *J. Phys. Chem. B* **2005**, *109*, 16011–16016.

[41] P. Kowalczyk, R. Holyst, M. Terrones, H. Terrones, *Phys. Chem. Chem. Phys.* **2007**, *9*, 1786–1792.

[42] J. W. Jang, C. E. Lee, C. I. Oh, C. J. Lee, *J. Appl. Phys.* **2005**, *98*, 074316–2/-3.

[43] N. B. McKeown, P. M. Budd, D. Book, *Macromol. Rapid Commun.* **2007**, *28*, 995–1002.

[44] N. L. Rosi, J. Eckert, M. Eddaoudi, D. T. Vodak, J. Kim, M. O'Keeffe, O. M. Yaghi, *Science* **2003**, *300*, 1127–1129.
[45] B. Chen, N. W. Ockwig, A. R. Millward, D. S. Contreras, O. M. Yaghi, *Angew. Chem.* **2005**, *117*, 4823–4827; *Angew. Chem. Int. Ed.* **2005**, *44*, 4745–4749.
[46] G. Férey, M. Latroche, C. Serre, F. Millange, T. Loiseau, A. Percheron-Guégan, *Chem. Commun.* **2003**, *24*, 2976–2977.
[47] M. Latroche, S. Suble, C. Serre, C. Mellot-Draznieks, P. L. Llewellyn, J.-H. Lee, J.-S. Chang, S. H. Jhung, G. Ferey, *Angew. Chem.* **2006**, *118*, 8407–8411; *Angew. Chem. Int. Ed.* **2006**, *45*, 8227–8231.
[48] Y. Liu, J. F. Eubank, A. J. Cairns, J. Eckert, V. C. Kravtsov, R. Luebke, M. Eddaoudi, *Angew. Chem.* **2007**, *119*, 3342–3347; *Angew. Chem. Int. Ed.* **2007**, *46*, 3278–3283.
[49] B. Panella, M. Hirscher, *Adv. Mater.* **2005**, *17*, 538–541.
[50] B. Kesanli, Y. Cui, M. R. Smith, E. W. Bittner, B. C. Brockrath, W. Lin, *Angew. Chem.* **2005**, *117*, 74–77; *Angew. Chem. Int. Ed.* **2005**, *44*, 72–75.
[51] Y. Li, F. H. Yang, R. T. Yang, *J. Phys. Chem. C* **2007**, *111*, 3405–3411.
[52] Y. Li, R. T. Yang, *AIChE J.* **2008**, *54*, 269–279.
[53] W. C. Conner, J. L. Falconer, *Chem. Rev.* **1995**, *95*, 759–788.
[54] G. M. Pajonk, *Appl. Catal. A* **2000**, *202*, 157–169.
[55] H. Furukawa, M. A. Miller, O. M. Yaghi, *J. Mater. Chem.* **2007**, *17*, 3197–3204.
[56] S. Ikeda, S. Ishino, T. Harada, N. Okamoto, T. Sakata, H. Mori, S. Kuwabata, T. Torimoto, M. Matsumura, *Angew. Chem.* **2006**, *118*, 7221–7224; *Angew. Chem. Int. Ed.* **2006**, *45*, 7063–7066.
[57] G. Sharma, Y. Mei, Y. Lu, M. Ballauff, T. Irrgang, S. Proch, R. Kempe, *J. Catal.* **2007**, *246*, 10–14.
[58] K. H. Park, K. Jang, H. J. Kim, S. U. Son, *Angew. Chem.* **2007**, *119*, 1170–1173; *Angew. Chem. Int. Ed.* **2007**, *46*, 1152–1155.
[59] A. Corma, P. Serna, H. Garcia, *J. Am. Chem. Soc.* **2007**, *129*, 6358–6359.
[60] R. D. Adams, E. M. Boswell, B. Captain, A. B. Hungria, P. A. Midgley, R. Raja, J. M. Thomas, *Angew. Chem.* **2007**, *119*, 8330–8333; *Angew. Chem. Int. Ed.* **2007**, *46*, 8182–8185.
[61] M. Boronat, P. Concepcion, A. Corma, S. Gonzalez, F. Illas, P. Serna, *J. Am. Chem. Soc.* **2007**, *129*, 16230–16237.
[62] V. Calo, N. Nacci, A. Monopoli, F. Montingelli, *J. Org. Chem.* **2005**, *70*, 6040–6044.
[63] Z. Zhang, Z. Zha, C. Gan, C. Pan, Y. Zhou, Z. Wang, M. Zhou, *J. Org. Chem.* **2006**, *71*, 4339–4342.
[64] Z. Zhang, Z. Wang, *J. Org. Chem.* **2006**, *71*, 7485–7487.
[65] J. G. de Vries, *Dalton Trans.* **2006**, 421–429.
[66] M. B. Thathagar, J. E. ten Elshof, G. Rothenberg, *Angew. Chem.* **2006**, *118*, 2952–2956; *Angew. Chem. Int. Ed.* **2006**, *45*, 2886–2890.
[67] K. Köhler, W. Kleist, S. S. Pröckl, *Inorg. Chem.* **2007**, *46*, 1876–1883.
[68] D. Astruc, *Inorg. Chem.* **2007**, *46*, 1884–1894.
[69] S. Proch, Y. Mei, J. M. Rivera Villanueva, Y. Lu, A. Karpov, M. Ballauff, R. Kempe, *Adv. Synth. Catal.* **2008**, *350*, 493–500.
[70] D. I. Enache, J. K. Edwards, P. Landon, B. Solsona-Espriu, A. F. Carley, A. A. Herzing, M. Watanabe, C. J. Kiely, D. W. Knight, G. J. Hutchings, *Science* **2006**, *311*, 362–365.
[71] A. Abad, P. Concepción, A. Corma, H. García, *Angew. Chem.* **2005**, *117*, 4134–4137; *Angew. Chem. Int. Ed.* **2005**, *44*, 4066–4069.
[72] H. Miyamura, R. Matsubara, Y. Miyazaki, S. Kobayashi, *Angew. Chem.* **2007**, *119*, 4229–4232; *Angew. Chem. Int. Ed.* **2007**, *46*, 4151–4154.
[73] T. Mitsudome, Y. Mikami, H. Funai, T. Mizugaki, K. Jitsukawa, K. Kaneda, *Angew. Chem.* **2008**, *120*, 144–147; *Angew. Chem. Int. Ed.* **2008**, *47*, 138–141.
[74] F.-Z. Su, Y.-M. Liu, L.-C. Wang, Y. Cao, H.-Y. He, K.-N. Fan, *Angew. Chem.* **2008**, *120*, 340–343; *Angew. Chem. Int. Ed.* **2008**, *47*, 334–337.
[75] M. Schrinner, S. Proch, Y. Mei, R. Kempe, N. Miyajima, M. Ballauff, *Adv. Mater.* **2008**, *20*, 1928–1933.
[76] T. Nishimura, N. Kakiuchi, M. Inoue, S. Uemura, *Chem. Commun.* **2000**, 1245–1246.
[77] N. Kakiuchi, T. Nishimura, M. Inoue, S. Uemura, *Bull. Chem. Soc. Jpn.* **2001**, *74*, 165–172.
[78] N. Kakiuchi, Y. Maeda, T. Nishimura, S. Uemura, *J. Org. Chem.* **2001**, *66*, 6620–6625.
[79] K. Mori, K. Yamaguchi, T. Hara, T. Mizugaki, K. Ebitani, K. Kaneda, *J. Am. Chem. Soc.* **2002**, *124*, 11572–11573.
[80] K. Mori, T. Hara, T. Mizugaki, K. Ebitani, K. Kaneda, *J. Am. Chem. Soc.* **2004**, *126*, 10657–10666.
[81] A. Abad, P. Concepción, A. Corma, H. García, *Angew. Chem.* **2005**, *117*, 4134–4137; *Angew. Chem. Int. Ed.* **2005**, *44*, 4066–4069.
[82] A. Abad, C. Almela, A. Corma, H. Garcia, *Tetrahedron* **2006**, *62*, 6666–6672.
[83] T. Mallat, A. Baiker, *Catal. Today* **1994**, *19*, 247–283.
[84] S. Zhang, X. Wu, M. Mehring, *Chem. Phys. Lett.* **1990**, *173*, 481–484.
[85] S. C. Shekar, A. Ramamoorthy, *Chem. Phys. Lett.* **2001**, *342*, 127–134; G. Metz, X. L. Wu, S. O. Smith, *J. Magn. Reson. Ser. A* **1994**, *110*, 219–227.
[86] B. M. Fung, A. K. Khitrin, K. Ermolaev, *J. Magn. Reson.* **2000**, *142*, 97–101.
[87] E. Weber, M. Hecker, E. Koepp, W. Orlia, M. Czugler, I. Csoregh, *J. Chem. Soc. Perkin Trans. 2* **1988**, 1251–1257.
[88] Z. Xue, M. J. Strouse, D. K. Shuh, C. B. Knobler, H. D. Kaesz, R. F. Hicks, R. S. Williams, *J. Am. Chem. Soc.* **1989**, *111*, 8779–8784.
[89] F. Sen, G. Gökagac, *J. Phys. Chem. C* **2007**, *111*, 5715–5720.
[90] B. D. Cullity, *Elements of X-ray Diffraction*, 2nd ed.; Addison-Wesley, London, **1978**, 101–102.
[91] H. K. Chae, D. Y. Siberio-Perez, J. Kim, Y.-B. Go, M. Eddaoudi, A. J. Matzger, M. O'Keeffe, O. M. Yaghi, *Nature* **2004**, *427*, 523–527.
[92] M. A. Miller, *DOE Annual Merit Review*, Washington DC, May 16, **2007**.
[93] R. Campesi, F. Cuevas, R. Gadiou, E. Leroy, M. Hirscher, C. Vix-Guterl, M. Latroche, *Carbon* **2008**, *46*, 206–214.
[94] S. Hayashi, *J. Alloys Compd.* **1997**, *248*, 66–69.
[95] Y. M. A. Yamada, T. Arakawa, H. Hocke, Y. Uozumi, *Angew. Chem.* **2007**, *119*, 718–720; *Angew. Chem. Int. Ed.* **2007**, *46*, 704–706.
[96] J. A. Greathouse, M. D. Allendorf, *J. Am. Chem. Soc.* **2006**, *128*, 10678–10679.

Received: May 29, 2008
Published online: July 30, 2008

